ELSEVIER

Journal of Organometallic Chemistry 582 (1999) 90–99

Journal of Organometallic Chemistry

# Some di- and tri-metal complexes derived from the synthon $[Ru(CO)_2(THF)(\eta^5\text{-}7,8\text{-}C_2B_9H_{11})]$☆

John C. Jeffery [a], Paul A. Jelliss [b], Gillian E.A. Rudd [b], Sumika Sakanishi [a], F. Gordon A. Stone [b,*], Jennifer Whitehead [a]

[a] *School of Chemistry, The University, Bristol BS8 1TS, UK*
[b] *Department of Chemistry, Baylor University, Waco, TX 76798-7348, USA*

Received 18 September 1998

**Abstract**

Treatment of THF solutions of $[Ru(CO)_2(THF)(\eta^5\text{-}7,8\text{-}C_2B_9H_{11})]$ (**2**) with $K[M(CO)_2(\eta^5\text{-}C_5H_5)]$ followed by addition of 18-crown-6 affords the salts $[K(18\text{-crown-6})][MRu(\mu\text{-}CO)_2(CO)_2(\eta^5\text{-}C_5H_5)(\eta^5\text{-}7,8\text{-}C_2B_9H_{11})]$ (**3a**, M = Fe; **3b**, M = Ru). The structure of **3a** was established by X-ray diffraction. In the anion of **3a** the Fe–Ru bond is symmetrically spanned by two CO groups, and each metal center carries a CO ligand terminally bound in a linear manner. The carbaborane and cyclopentadienyl ligands have a *cis* disposition with respect to each other. The potassium ion of the $[K(18\text{-crown-6})]^+$ moiety is ligated by an oxygen atom of one of the μ-CO groups. The reaction of **2** with $[Rh_2(\mu\text{-}CO)_2(\eta^5\text{-}C_5Me_5)_2]$ in THF yields a chromatographically separable mixture of the di- and tri-metal species $[RuRh(\mu\text{-}H)(\mu\text{-}\sigma,\eta^5\text{-}7,8\text{-}C_2B_9H_{10})(CO)_3(\eta^5\text{-}C_5Me_5)]$ (**4**) and $[RuRh_2(\mu\text{-}CO)_3(\mu_3\text{-}CO)(\eta^5\text{-}C_5Me_5)_2(\eta^5\text{-}7,8\text{-}C_2B_9H_{11})]$ (**5**). An X-ray diffraction study of **5** revealed a molecular structure based on a triangular array of metal atoms with the Ru atom and the Rh atoms pentahapto coordinated by $7,8\text{-}C_2B_9H_{11}$ and $C_5Me_5$ ligands, respectively. The metal triangle is symmetrically capped by a CO group. The Rh–Rh bond is symmetrically bridged by a CO ligand, while the two Ru–Rh bonds are each asymmetrically bridged by a CO molecule. The NMR ($^1H$-, $^{13}C\{^1H\}$-, and $^{11}B\{^1H\}$-) data for the new compounds are reported and discussed in relation to their structures. 

*Keywords:* Boron; Carbaborane; Ruthenium; Iron; Rhodium

## 1. Introduction

Organoruthenium complexes containing the $\eta^5\text{-}C_5H_5$ group have been studied extensively, and this area continues to be an active one for research [1]. In contrast the corresponding chemistry of species in which the metal is coordinated by the related $\eta^5\text{-}7,8\text{-}C_2B_9H_{11}$ ligand is at present much less developed[1]. This situation has arisen because convenient syntheses of complexes containing the $Ru(\eta^5\text{-}7,8\text{-}C_2B_9H_{11})$ moiety which can themselves be used as a precursor to other compounds were not available until recently [2–6].

We have developed [2] a high yield synthesis of the complex salt $[NEt_4][RuI(CO)_2(\eta^5\text{-}7,8\text{-}C_2B_9H_{11})]$ (**1**)

☆ Dedicated to Professor Alan H. Cowley on the occasion of his 65th birthday.

* Corresponding author.
*E-mail address:* gordon-stone@baylor.edu (F.G.A. Stone)

[1] The compounds described in this paper have a ruthenium atom incorporated into a *closo*-1,2-dicarba-3-ruthenadodecaborane structure. However, to avoid a complicated nomenclature for the complexes reported, and to relate them to the many known ruthenium species with $\eta^5$-coordinated cyclopentadienyl ligands, we treat the cages as *nido*-11-vertex ligands with numbering as for an icosahedron from which the 12th vertex has been removed.

0022-328X/99/$ - see front matter 
PII: S0022-328X(98)01190-5

Table 1
Analytical and physical data

| Compound | Colour | Yield (%) | $\nu_{max}$(CO)[a] ($cm^{-1}$) | Analysis (%)[b] | |
|---|---|---|---|---|---|
| | | | | C | H |
| [K(18-crown-6)][*cis*-FeRu(μ-CO)$_2$(CO)$_2$(η$^5$-$C_5H_5$)(η$^5$-7,8-$C_2B_9H_{11}$)] (**3a**) | Red | 21 | 1988 s, 1946 s, 1760 s | 35.7 (35.9) | 5.2 (5.2) |
| [K(18-crown-6)][*cis*-Ru$_2$(μ-CO)$_2$(CO)$_2$(η$^5$-$C_5H_5$)(η$^5$-7,8-$C_2B_9H_{11}$)] (**3b**) | Yellow | 20 | 1988 s, 1946 s, 1760 s | 33.7 (33.9) | 5.0 (5.0) |
| [RuRh(μ-H)(μ-σ,η$^5$-7,8-$C_2B_9H_{10}$)(CO)$_3$(η$^5$-$C_5Me_5$)] (**4**)[c] | Red | 15 | 2035 vs, 2017 vs, 1979 s | | |
| [RuRh$_2$(μ-CO)$_3$(μ$_3$-CO)(η$^5$-$C_5Me_5$)$_2$(η$^5$-7,8-$C_2B_9H_{11}$)] (**5**) | Dark green | 38 | 1890 s, 1852 m, 1819 m, 1680 m br | 37.3 (38.0) | 5.0 (5.0) |

[a] Measured in $CH_2Cl_2$. All complexes show a broad medium-intensity band at ca. 2550 $cm^{-1}$ due to cage B–H absorptions.
[b] Calculated values are given in parentheses.
[c] Compound **4** is an oily solid which is difficult to purify. FAB MS: $m/z$ 556.04 (**4**, calc. 555.64), 528.03 (**4** –CO), 500.04 (**4** –CO × 2).

from [Ru(CO)$_3$(η$^5$-7,8-$C_2B_9H_{11}$)], a complex first reported by Behnken and Hawthorne [7]. This salt can be used to generate in situ the reactive synthon [Ru(CO)$_2$(THF)(η$^5$-7,8-$C_2B_9H_{11}$)] (**2**) by reaction with $AgBF_4$ in THF. Details of subsequent reactions of **2** with platinum species [2], organic molecules [3], and alkylidyne complexes of molybdenum and tungsten [4] have been recently described. We report here, novel di- and trinuclear metal complexes obtained using the reagent **2**.

## 2. Results and discussion

Treatment of THF solutions of compound **2** with K[M(CO)$_2$(η$^5$-$C_5H_5$)], followed by addition of 18-crown-6 yielded the salts [K(18-crown-6)][*cis*-MRu(μ-CO)$_2$(CO)$_2$(η$^5$-$C_5H_5$)(η$^5$-7,8-$C_2B_9H_{11}$)] (**3a**, M = Fe; **3b**, M = Ru), data for which are given in Tables 1 and 2. Complex **3a** was structurally characterized by X-ray diffraction and the results of this study are presented before discussion of the spectroscopic data for this species. Selected bond lengths and angles are given in Table 3 and the structure is displayed in Fig. 1.

The Fe(1)–Ru(1) contact [2.6559(9) Å] is comparable with that found [2.626(1) Å] for the metal–metal bond in the neutral complex [*trans*-FeRu(μ-CO)$_2$(CO)$_2$(η$^5$-$C_5H_5$)$_2$] (**B**, Scheme 1) [8]. Evidently the additional negative charge associated with the iron–ruthenium fragment in complex **3a** has little effect on the Fe–Ru distance. This is unsurprising since the charge in such species is delocalised within the carbaborane cage framework [9]. The metal–metal bond in **3a** is symmetrically bridged by two CO ligands [Ru(1)–C av. 2.032, Fe(1)–C av. 1.946 Å] as is found in complex **B**, and also in the homonuclear dimetal compounds [M$_2$(μ-CO)$_2$(CO)$_2$(η$^5$-$C_5H_5$)$_2$] (*trans*-**A**, M = Fe [10,11]; *cis*-**A**, M = Fe [10,12]; *trans*-**C**, M = Ru [13,14]) and in the di-iron complex Cs$_2$[*cis*-Fe$_2$(μ-CO)$_2$(CO)$_2$(η$^5$-7,8-$C_2B_9H_{11}$)$_2$] (**D**) [15]. For comparative purposes all these structurally related molecules are displayed in Scheme 1. Also depicted is the complex salt [K(18-crown-6)]$_2$[*trans*-Ru$_2$(μ-CO)$_2$(CO)$_2$(η$^5$-7,8-$C_2B_9H_{11}$)$_2$] (**E**) [7], which has not been structurally characterized by X-ray diffraction. A brief qualitative discussion of the nature of these various species is given later.

Two carbonyl ligands of **3a** are clearly bound to their respective metal centers in a terminal and linear manner [Ru(1)–C(12)–O(12) 177.5(4), Fe(1)–C(15)–O(15) 178.8(4)°]. The two Ru–μ-C–Fe planes are inclined to one another at an angle of 164° about the Ru–Fe axis. This arrangement is identical with that observed for the *cis* isomer of complex **A** [12], and for the dianion **D** which also has a *cis* configuration for its pentahapto coordinated ligands [15]. Molecular orbital considerations have accounted for this structural feature [10]. The distortion allows an increase in overlap between π* orbitals of the μ-CO ligands and the metal atoms, and a similar situation is envisaged for the anion of **3a**. A very interesting feature is the presence of a bond between the bridging carbonyl oxygen O(13) and the potassium ion of the [K(18-crown-6)]$^+$ moiety [K(1)···O(13) 2.759(3) Å]. This distance is very close in magnitude to the sum (2.83 Å) of the ionic radius for potassium (1.33 Å [16]) and the van der Waals radius for oxygen (ca. 1.50 Å [17]). Interactions between oxygen atoms of terminal carbonyl groups and alkali metal ions (usually encapsulated by crown ethers) are well established [18–21] in transition metal carbonyl complexes. The origin of such bonding in solution and in the solid state has been attributed to attraction between the alkali metal cation and the carbonyl oxygen atom and also to a direct interaction between the alkali metal ion and the transition metal [18]. There is, however, no

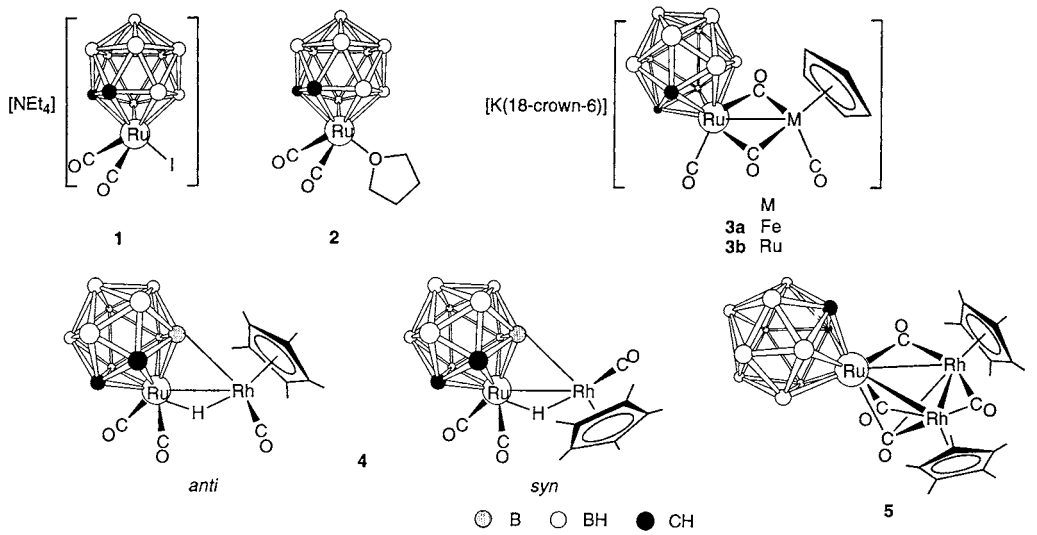


evidence of any interaction in **3a** between the K(1) atom and either the Fe(1) or Ru(1) atoms, this being supported by the near-linear angle K(1)–O(13)–C(13) of 167.6(3)°. Furthermore, we have found no report of such bonding between a 'bridging' carbonyl oxygen atom and a crown-ether-complexed alkali metal ion in either the open literature or by search of the Cambridge Crystallographic Database. On the opposite side of the $[K(18\text{-crown-6})]^+$ moiety to the FeRu molecular anion, there is a long contact [2.909(3) Å] between K(1) and an oxygen atom (O21′) of the second $[K(18\text{-crown-6})]^+$ fragment in the unit cell.

In complex **3a** of special note is the *cis* disposition of the carbaborane cage with respect to the cyclopentadienyl ligand. Three CO stretching absorptions are observed at 1988, 1946 and 1760 $cm^{-1}$ in the IR spectrum measured in $CH_2Cl_2$ (Table 1). The latter band must correspond to the antisymmetric stretch of the μ-CO ligands, while the remaining two absorptions are due to the *cis* terminal CO groups, observations in agreement with the results of the X-ray diffraction study. The $^1H$- and $^{11}B\{^1H\}$-NMR spectra are simple and not very informative with regard to the structure of the anion in solution. The $^{13}C\{^1H\}$-NMR spectrum measured at ambient temperatures revealed only peaks due to the carbon atoms of the cyclopentadienyl, carbaborane cage and 18-crown-6 fragments. The absence of CO resonances indicated that the complex was at or near the coalescence temperature for a fluxional process, one most likely involving site exchange of the carbonyl

Table 2
$^1H$-, $^{13}C$- and $^{11}B$-NMR data[a]

| Compound | $^1H$ ($\delta$)[b] | $^{13}C$ ($\delta$)[c] | $^{11}B$ ($\delta$)[d] |
|---|---|---|---|
| **3a**[e] | 2.14 (s, 2 H, cage CH), 3.61 (s, 24 H, 18-crown-6), 4.75 (s, 5 H, $C_5H_5$) | 261.6 (μ-CO), 212.3 (FeCO), 197.8 (RuCO), 86.6 ($C_5H_5$), 69.5 (18-crown-6), 42.4 (cage CH) | −0.2 (1 B), −9.0 (3 B), −10.8 (2 B), −21.0 (3 B) |
| **3b**[e] | 2.19 (s, 2 H, cage CH), 3.64 (s, 24 H, 18-crown-6), 5.26 (s, 5 H, $C_5H_5$) | 248.3 (μ-CO), 200.2, 198.1 (CO), 89.1 ($C_5H_5$), 69.5 (18-crown-6), 42.9 (cage CH) | −0.7 (1 B), −7.8 (1 B), −9.0 (2 B), −10.7 (2 B), −20.9 (3 B) |
| **4**[f] | −14.96* [d, 1 H, μ-H, $J$(RhH) 24], −14.74 [d, 1 H, μ-H, $J$(RhH) 24], 1.98* (s, 15 H, Me), 2.02 (s, 15 H, Me), 2.62 (s br, 1 H, cage CH), 2.89*, 3.50* (s br × 2, 2 H, cage CH), 3.58 (s br, 1 H, cage CH) | 196.8, 194.7 (RuCO), 191.5 [d, RhCO, $J$(RhC) 79], 106.9 [d, $C_5Me_5$, $J$(RhC) 4], 105.3* [d, $C_5Me_5$, $J$(RhC) 4], 44.6, 41.8*, 37.7*, 36.7 (cage CH), 10.7, 10.6* ($C_5Me_5$) | 41.8 (1 B, B–Rh), 40.0* (1 B, B–Rh), 1.3 (1 B), −1.4 (2 B), −8.5* (1 B), −11.5 (1 B), −15.0 (1 B), −16.6 (2 B), −27.7 (1 B) |
| **5**[g] | 1.73 (s, 30 H, Me), 2.56 (s, 2 H, cage CH) | 109.0 (m br, $C_5Me_5$), 8.7 ($C_5Me_5$) | 9.3 (1 B), 0.1 (1 B), −4.3 (2 B), −8.3 (2 B), −15.7 (2 B), −20.0 (1 B) |

[a] Chemical shifts ($\delta$) in ppm, coupling constants ($J$) in Hz, measurements in $CD_2Cl_2$, and at r.t. unless otherwise stated.
[b] Resonances for terminal BH protons occur as broad unresolved signals in the range $\delta$ ca. −2 to 3.
[c] $^1H$ decoupled, chemical shifts are positive to high frequency of $SiMe_4$.
[d] $^1H$ decoupled, chemical shifts are positive to high frequency of $BF_3 \cdot Et_2O$ (external).
[e] $^{13}C\{^1H\}$-NMR spectrum was recorded at −80°C.
[f] Peaks marked with an asterisk correspond to signals for the minor isomer (see text).
[g] Due to poor solubility, signals due to carbonyl and cage carbon nuclei were not observed in the $^{13}C\{^1H\}$-NMR spectrum.

Table 3
Selected bond lengths (Å) and bond angles (°) for [K(18-crown-6)][*cis*-FeRu(μ-CO)$_2$(CO)$_2$($\eta^5$-$C_5H_5$)($\eta^5$-7,8-$C_2B_9H_{11}$)] (**3a**) with estimated S.D. in parentheses

| | | | | | | | |
|---|---|---|---|---|---|---|---|
| *Bond lengths* (Å) | | | | | | | |
| Ru(1)–C(12) | 1.861(4) | Ru(1)–C(14) | 2.007(4) | Ru(1)–C(13) | 2.057(4) | Ru(1)–C(2) | 2.262(4) |
| Ru(1)–B(5) | 2.262(4) | Ru(1)–C(1) | 2.282(4) | Ru(1)–B(3) | 2.305(4) | Ru(1)–B(4) | 2.318(5) |
| Ru(1)–Fe(1) | 2.6559(9) | Fe(1)–C(15) | 1.752(4) | Fe(1)–C(13) | 1.900(4) | Fe(1)–C(14) | 1.992(4) |
| Fe(1)–C(19) | 2.076(4) | Fe(1)–C(20) | 2.106(4) | Fe(1)–C(18) | 2.115(4) | Fe(1)–C(16) | 2.134(4) |
| Fe(1)–C(17) | 2.135(4) | C(12)–O(12) | 1.151(5) | C(13)–O(13) | 1.179(5) | O(13)–K(1) | 2.759(3) |
| C(14)–O(14) | 1.173(5) | C(15)–O(15) | 1.151(5) | K(1)–O(30) | 2.671(3) | K(1)–O(33) | 2.760(4) |
| K(1)–O(24) | 2.782(3) | K(1)–O(36) | 2.811(3) | K(1)–O(21) | 2.865(3) | K(1)–O(27) | 2.873(3) |
| K(1)–O(21′) | 2.909(3) | | | | | | |
| *Bond angles* (°) | | | | | | | |
| C(12)–Ru(1)–C(14) | 86.0(2) | C(12)–Ru(1)–C(13) | 91.4(2) | C(14)–Ru(1)–C(13) | 92.7(2) | | |
| C(12)–Ru(1)–C(2) | 158.6(2) | C(14)–Ru(1)–C(2) | 115.25(14) | C(13)–Ru(1)–C(2) | 89.95(14) | | |
| C(12)–Ru(1)–B(5) | 87.0(2) | C(14)–Ru(1)–B(5) | 146.0(2) | C(13)–Ru(1)–B(5) | 120.7(2) | | |
| C(2)–Ru(1)–B(5) | 74.1(2) | C(12)–Ru(1)–C(1) | 117.3(2) | C(14)–Ru(1)–C(1) | 156.73(14) | | |
| C(13)–Ru(1)–C(1) | 87.1(2) | C(2)–Ru(1)–C(1) | 41.51(13) | B(5)–Ru(1)–C(1) | 44.1(2) | | |
| C(12)–Ru(1)–B(3) | 141.6(2) | C(14)–Ru(1)–B(3) | 87.5(2) | C(13)–Ru(1)–B(3) | 126.7(2) | | |
| C(2)–Ru(1)–B(3) | 44.1(2) | B(5)–Ru(1)–B(3) | 77.7(2) | C(1)–Ru(1)–B(3) | 74.2(2) | | |
| C(12)–Ru(1)–B(4) | 99.2(2) | C(14)–Ru(1)–B(4) | 102.2(2) | C(13)–Ru(1)–B(4) | 162.3(2) | | |
| C(2)–Ru(1)–B(4) | 75.1(2) | B(5)–Ru(1)–B(4) | 46.5(2) | C(1)–Ru(1)–B(4) | 75.5(2) | | |
| B(3)–Ru(1)–B(4) | 45.8(2) | C(12)–Ru(1)–Fe(1) | 95.35(13) | C(14)–Ru(1)–Fe(1) | 48.15(12) | | |
| C(13)–Ru(1)–Fe(1) | 45.39(11) | C(2)–Ru(1)–Fe(1) | 100.71(10) | B(5)–Ru(1)–Fe(1) | 165.83(13) | | |
| C(1)–Ru(1)–Fe(1) | 123.92(10) | B(3)–Ru(1)–Fe(1) | 108.03(12) | B(4)–Ru(1)–Fe(1) | 145.85(13) | | |
| C(15)–Fe(1)–C(13) | 91.0(2) | C(15)–Fe(1)–C(14) | 90.8(2) | C(13)–Fe(1)–C(14) | 98.1(2) | | |
| C(15)–Fe(1)–C(19) | 91.1(2) | C(13)–Fe(1)–C(19) | 136.4(2) | C(14)–Fe(1)–C(19) | 125.4(2) | | |
| C(15)–Fe(1)–C(20) | 107.0(2) | C(13)–Fe(1)–C(20) | 99.0(2) | C(14)–Fe(1)–C(20) | 155.0(2) | | |
| C(19)–Fe(1)–C(20) | 39.4(2) | C(15)–Fe(1)–C(18) | 113.0(2) | C(13)–Fe(1)–C(18) | 154.1(2) | | |
| C(14)–Fe(1)–C(18) | 91.4(2) | C(19)–Fe(1)–C(18) | 39.3(2) | C(20)–Fe(1)–C(18) | 65.8(2) | | |
| C(15)–Fe(1)–C(16) | 145.0(2) | C(13)–Fe(1)–C(16) | 90.0(2) | C(14)–Fe(1)–C(16) | 123.7(2) | | |
| C(19)–Fe(1)–C(16) | 65.1(2) | C(20)–Fe(1)–C(16) | 38.6(2) | C(18)–Fe(1)–C(16) | 64.9(2) | | |
| C(15)–Fe(1)–C(17) | 151.7(2) | C(13)–Fe(1)–C(17) | 116.8(2) | C(14)–Fe(1)–C(17) | 90.8(2) | | |
| C(19)–Fe(1)–C(17) | 65.3(2) | C(20)–Fe(1)–C(17) | 65.2(2) | C(18)–Fe(1)–C(17) | 38.6(2) | | |
| C(16)–Fe(1)–C(17) | 38.7(2) | C(15)–Fe(1)–Ru(1) | 99.21(14) | C(13)–Fe(1)–Ru(1) | 50.41(12) | | |
| C(14)–Fe(1)–Ru(1) | 48.63(12) | C(19)–Fe(1)–Ru(1) | 167.80(14) | C(20)–Fe(1)–Ru(1) | 140.24(12) | | |
| C(18)–Fe(1)–Ru(1) | 129.25(14) | C(16)–Fe(1)–Ru(1) | 108.12(11) | C(17)–Fe(1)–Ru(1) | 102.95(12) | | |
| O(12)–C(12)–Ru(1) | 177.5(4) | O(13)–C(13)–Fe(1) | 141.4(3) | O(13)–C(13)–Ru(1) | 133.9(3) | | |
| Fe(1)–C(13)–Ru(1) | 84.2(2) | C(13)–O(13)–K(1) | 167.6(3) | O(14)–C(14)–Fe(1) | 135.0(3) | | |
| O(14)–C(14)–Ru(1) | 141.7(3) | Fe(1)–C(14)–Ru(1) | 83.2(2) | O(15)–C(15)–Fe(1) | 178.8(4) | | |

ligands between the two metal centers. In complex **B** this process, observed at ambient temperatures, is coupled with a *cis–trans* interconversion [8], one singlet being observed for the CO carbon nuclei. Upon cooling to −80°C, a set of intense sharp signals was observed and attributed to the dominant *trans* isomer and a weaker broad signal to the *cis* species, the latter still undergoing CO exchange at this temperature. Indeed, with all the complexes A–C, both *cis* and *trans* isomers have been observed in solution along with a transient non-bridged species [10]. A variable temperature $^{13}C\{^1H\}$-NMR study of complex **3a** was therefore undertaken. A spectrum recorded at −80°C revealed only a single set of intense peaks at $\delta$ 261.6 (μ-CO), 212.3 (FeCO) and 197.8 (RuCO), the chemical shift assignments being based on the previous analysis for **B** [8]. Thus complex **3a** appears to be limited to a single geometric configuration in solution at −80°C, proba-

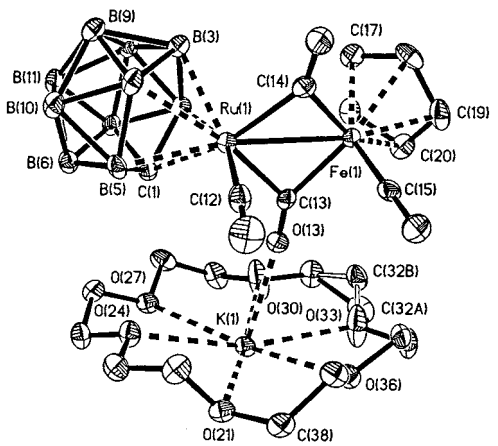


Fig. 1. Structure of [K(18-crown-6)][FeRu(μ-CO)$_2$(CO)$_2$($\eta^5$-$C_5H_5$)($\eta^5$-7,8-$C_2B_9H_{11}$)] (**3a**), showing the crystallographic labelling scheme. Hydrogen atoms are omitted for clarity and thermal ellipsoids are shown at the 40% probability level.

bly that found in the X-ray structure determination, i.e. with a *cis* arrangement of the $\eta^5$-7,8-$C_2B_9H_{11}$ and $\eta^5$-$C_5H_5$ ligands.

As mentioned above, the bisferracarbaborane complex **D** (Scheme 1) was similarly found to exist in the *cis* geometry as revealed by X-ray analysis [15] and by its IR spectrum measured in Nujol [22]. However, spectra recorded in MeCN solutions suggested the *trans* form may be prevalent in this solvent. No variable temperature NMR experiments have been reported for **D** to examine the possible extent of fluxionality. Evidence from the IR spectrum (Nujol mull) for the analogous diruthenium complex **E**, however, suggests that only the *trans* isomer exists in the solid state since only one terminal $\nu_{max}$(CO) absorption band (1910 $cm^{-1}$) is observed [7]. We were therefore interested to investigate the nature of a cyclopentadienyl–carbaborane diruthenium species. As mentioned above, the salt **3b** was synthesized in a similar manner to **3a**, using K[Ru(CO)$_2$($\eta^5$-$C_5H_5$)]. As with **3a**, the $^1$H- and $^{11}$B{$^1$H}-NMR spectra of **3b** are not structurally informative and the $^{13}$C{$^1$H}-NMR spectrum again showed no resonances, broad or otherwise, due to the carbonyl carbon nuclei, implying dynamic behavior. Reducing the temperature to $-80$°C resulted in a $^{13}$C{$^1$H}-NMR spectrum strikingly similar to that of **3a**, with sharp resonances at $\delta$ 248.3 due to the bridging CO and at 202.2 and 198.1 arising from the terminal CO ligands. Most importantly, the IR spectrum of **3b** (Table 1) is identical with that of **3a**. Clearly a *cis* form of **3b** is undergoing slow CO exchange at room temperature (r.t.), and this interconversion can be successfully frozen out by cooling to $-80$°C. Again there is no evidence for a *trans* isomer of **3b**, and for neither of the complexes **3** are there spectroscopic indications of non-bridged species.

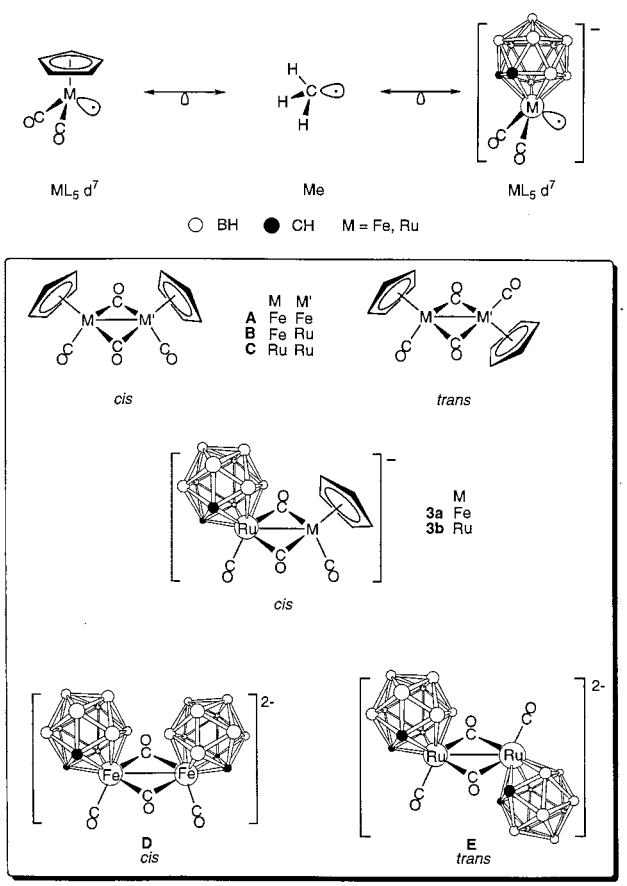


Scheme 1. Isolobal mapping of the complexes **3** with the known molecules **A**–**E**.

The existence of complexes **3** and **A**–**E** can be rationalized in terms of the isolobal mapping shown in Scheme 1, [23]. These molecules can be regarded as resulting from a combination of two $ML_5$ $d^7$ methyl-like radicals, with the obvious additional complication of the bridging carbonyls; a feature, nevertheless, common to all the compounds concerned. What is more difficult to understand is the preference for one geometrical isomer over the other, i.e. *cis* or *trans*. The relative energies of the isomers of the complexes **A** and **C** have been discussed elsewhere [24]. The structural similarities between the *cisoid* complexes **3a**, *cis*-**A** and -**D** in terms of the metal–carbonyl framework suggest steric factors are not dominant in determining the nature of the complexes. The fact that complex **E** has an apparent overall *transoid* preference while **3** and **D** are almost exclusively *cis* is perplexing, and we can only assume subtle electronic effects are at play, the nature of which are as yet, unclear.

It had been hoped that the molecules **3** would themselves be employed as precursors to new compounds since it is known that the oxygen atoms of the bridging carbonyl ligands in complexes **A** and **C** are susceptible to attack by Lewis acids [10,13]. Alas, treatment of both **3a** and **3b** with sources of $H^+$ and $Me^+$ under a variety of conditions led only to complete decomposition.

There have been a limited number of studies on mixed-metal ruthenium–rhodium cluster molecules. Generally these involve neutral complexes which contain hydrido, phosphine or cyclopentadienyl ligands, with a small amount of research into charged homoleptic species of the type $[Ru_nRh_m(CO)_x]^{y-}$ ($n = 1$–3, $m = 1$–5, $x = 12$–16, $y = 1,2$) [25–28]. We have used the reagent **2** to prepare ruthenium–rhodium molecules by treatment with the dimer [Rh$_2$($\mu$-CO)$_2$($\eta^5$-$C_5Me_5$)$_2$] in THF. Two complexes were isolated from this reaction. The first to be eluted from the chromatography column and successfully identified was the neutral dimetal species [RuRh($\mu$-H)($\mu$-$\sigma$,$\eta^5$-7,8-$C_2B_9H_{10}$)(CO)$_3$-($\eta^5$-$C_5Me_5$)] (**4**). Although tractable crystals of **4** could not be grown for an X-ray diffraction study, the structure could be confidently assigned through analysis of the IR and NMR spectra.

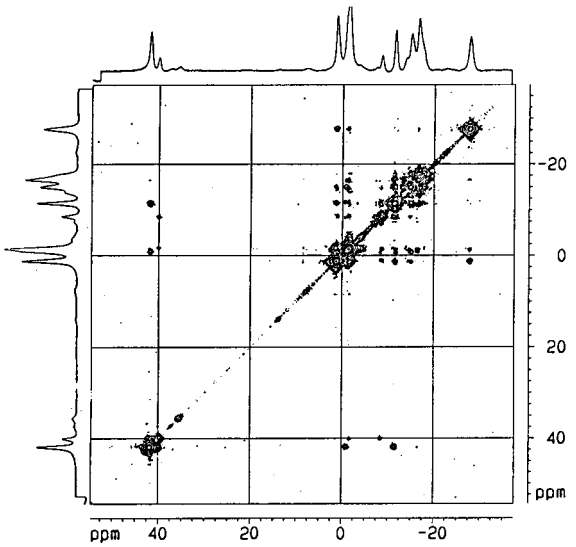


Fig. 2. The $^{11}B\{^1H\}-^{11}B\{^1H\}$-COSY 115.55 MHz NMR spectrum of compound **4**.

The IR spectrum of **4** displayed three CO stretching bands in the terminal range (Table 1), as one might expect for an asymmetrical molecule with two carbonyl ligands carried by the Ru atom and one by the Rh atom. The $^1H$-NMR spectrum revealed a diagnostic doublet resonance at $\delta$ −14.74 with $J(RhH) = 24$ Hz, the chemical shift being typical for a hydrido ligand bridging a metal–metal bond [29]. This resonance was accompanied by a singlet peak for the $\eta^5$-$C_5Me_5$ ligand ($\delta$ 2.02) and two singlets for the cage C–H protons ($\delta$ 2.62 and 3.58) in accord with the asymmetry of the molecule due to the absence of a mirror plane. The $^{13}C\{^1H\}$-NMR spectrum was also revealing with two of three CO signals appearing as singlets ($\delta$ 196.8 and 194.7) and the third as a doublet [$\delta$ 191.5, $J(RhC) = 79$ Hz]. This enabled us to ascribe the latter resonance as due to a rhodium-bound CO ligand, and the other two to the inequivalent RuCO ligands. From the $^1H$- and $^{13}C\{^1H\}$-NMR spectra it was also possible to identify the presence of a minor species in solution. Thus in the $^1H$-NMR spectrum there was a weak doublet at $\delta$ −14.96 [$J(RhH) = 24$ Hz] and broad singlet peaks for the cage CH protons at $\delta$ 2.89 and 3.50. Peak integrals indicated a 5:1 ratio of major to minor isomers. In the $^{13}C\{^1H\}$-NMR spectrum, although no peaks could be assigned to the CO groups of the minor species, signals due to the $\eta^5$-$C_5Me_5$ and cage CH carbon nuclei were clearly visible. The $^{11}B\{^1H\}$-NMR spectrum of **4** showed diagnostic peaks at $\delta$ 41.8 and 40.0 (ratio 5:1) due to the BRh boron nuclei of the major and minor isomers, respectively. These signals remain as singlets in the fully coupled $^{11}B$-NMR spectrum.

The precise structure of the molecule **4** is dependent upon two variables: (i) whether the exopolyhedral B–Rh σ bond involves a boron atom α (CC*B*BB) or β (CC*B*BB) to a cage carbon atom in the ligating belt of the cage, and (ii) the disposition of the $\eta^5$-$C_5Me_5$ group with respect to the B–Rh bond and its neighboring cage carbon atoms. In the above-mentioned absence of an X-ray structural determination an $^{11}B\{^1H\}-^{11}B\{^1H\}$-COSY-NMR spectrum (Fig. 2) proved to be very useful as an analytical probe. Of primary concern are the correlations with the distinctive BRh resonances of the major ($\delta$ 41.8) and minor ($\delta$ 40.0) isomers. The remainder of the off-diagonal peaks will not be discussed. The former peak, due to the major species, correlates with two resonances in the $\delta$ +1 to −30 range, one of which integrates to 2 B. This clearly implies that the α boron must be the cage vertex engaged in the exopolyhedral bond to the rhodium atom, as this has a connectivity to three other cage boron atoms (the β boron atom having a connectivity of four). We therefore designate the major species as the α-isomer, **4a**. The minor species naturally gives rise to weaker off-diagonal correlations, which makes confirmation of its structure somewhat tenuous. However, only two peaks are observed, which suggests that the minor species is likely to be **4b**, the isomer of **4a** where the $\eta^5$-$C_5Me_5$ ligand lies on the opposite side of the rhodium atom. Thus **4a** and **4b** are *syn* and *anti* isomers depending on whether the $\eta^5$-$C_5Me_5$ ligand lies on the same or on opposite sides of the molecule as the cage carbon atoms, both isomers having $B_\alpha$–Rh linkages. However, unfortunately NMR experiments could not distinguish exactly which isomer (**4a** or **4b**) is the *syn* and which is the *anti* form. There is almost certainly no exchange of the kind **4a** ⇌ **4b** in solution, though the complexes are inseparable on a chromatography column.

A second product of the reaction between **2** and $[Rh_2(\mu\text{-}CO)_2(\eta^5\text{-}C_5Me_5)_2]$ was removed from the chromatography column and identified as $[RuRh_2(\mu$-

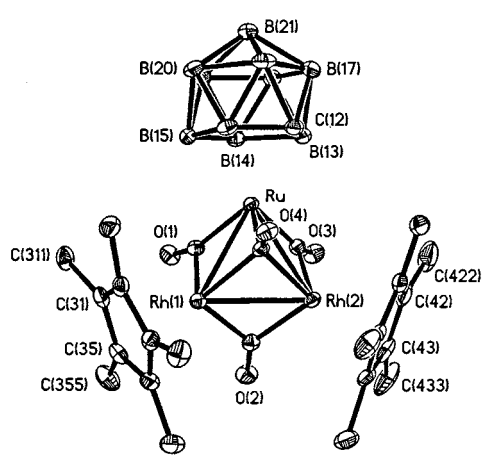


Fig. 3. Structure of $[RuRh_2(\mu\text{-}CO)_3(\mu_3\text{-}CO)(\eta^5\text{-}C_5Me_5)_2(\eta^5\text{-}7,8\text{-}C_2B_9H_{11})]$ (**5**), showing the crystallographic labelling scheme. Hydrogen atoms are omitted for clarity and thermal ellipsoids are shown at the 40% probability level.

Table 4
Selected bond lengths (Å) and bond angles (°) for $[RuRh_2(\mu\text{-}CO)_3(\mu_3\text{-}CO)(\eta^5\text{-}C_5Me_5)_2(\eta^5\text{-}7,8\text{-}C_2B_9H_{11})]$ (**5**) with estimated S.D. in parentheses

| | | | | | | | |
|---|---|---|---|---|---|---|---|
| *Bond lengths* (Å) | | | | | | | |
| Ru–C(3) | 1.954(2) | Ru–C(1) | 1.954(2) | Ru–C(4) | 2.120(2) | Ru–B(15) | 2.259(3) |
| Ru–B(13) | 2.260(3) | Ru–C(12) | 2.279(2) | Ru–B(14) | 2.286(3) | Ru–C(11) | 2.295(2) |
| Ru–Rh(1) | 2.7600(5) | Ru–Rh(2) | 2.7735(4) | Rh(1)–C(2) | 2.032(2) | Rh(1)–C(4) | 2.094(2) |
| Rh(1)–C(1) | 2.180(2) | Rh(1)–C(34) | 2.220(2) | Rh(1)–C(35) | 2.233(2) | Rh(1)–C(31) | 2.237(2) |
| Rh(1)–C(32) | 2.260(2) | Rh(1)–C(33) | 2.280(2) | Rh(1)–Rh(2) | 2.7030(5) | Rh(2)–C(2) | 2.017(2) |
| Rh(2)–C(4) | 2.082(2) | Rh(2)–C(3) | 2.203(2) | Rh(2)–C(42) | 2.222(2) | Rh(2)–C(44) | 2.226(2) |
| Rh(2)–C(43) | 2.228(2) | Rh(2)–C(41) | 2.256(2) | Rh(2)–C(45) | 2.285(2) | C(1)–O(1) | 1.163(3) |
| C(2)–O(2) | 1.169(3) | C(3)–O(3) | 1.165(3) | C(4)–O(4) | 1.192(3) | C(31)–C(35) | 1.422(3) |
| C(31)–C(32) | 1.444(3) | C(32)–C(33) | 1.413(3) | C(33)–C(34) | 1.443(3) | C(34)–C(35) | 1.442(3) |
| C(41)–C(45) | 1.401(4) | C(41)–C(42) | 1.448(4) | C(42)–C(43) | 1.411(4) | C(43)–C(44) | 1.442(4) |
| C(44)–C(45) | 1.441(3) | | | | | | |
| *Bond angles* (°) | | | | | | | |
| C(3)–Ru–C(1) | 81.29(10) | C(3)–Ru–C(4) | 100.22(9) | C(1)–Ru–C(4) | 100.39(9) | | |
| C(3)–Ru–Rh(1) | 91.25(7) | C(1)–Ru–Rh(1) | 51.72(7) | C(4)–Ru–Rh(1) | 48.68(6) | | |
| C(3)–Ru–Rh(2) | 52.10(7) | C(1)–Ru–Rh(2) | 90.98(7) | C(4)–Ru–Rh(2) | 48.12(6) | | |
| Rh(1)–Ru–Rh(2) | 58.481(12) | C(2)–Rh(1)–C(4) | 97.27(9) | C(2)–Rh(1)–C(1) | 80.11(9) | | |
| C(4)–Rh(1)–C(1) | 94.21(9) | C(2)–Rh(1)–Rh(2) | 47.90(7) | C(4)–Rh(1)–Rh(2) | 49.48(6) | | |
| C(1)–Rh(1)–Rh(2) | 88.24(6) | C(2)–Rh(1)–Ru | 87.40(7) | C(4)–Rh(1)–Ru | 49.49(6) | | |
| C(1)–Rh(1)–Ru | 44.72(6) | Rh(2)–Rh(1)–Ru | 61.009(13) | C(2)–Rh(2)–C(4) | 98.11(9) | | |
| C(2)–Rh(2)–C(3) | 79.82(9) | C(4)–Rh(2)–C(3) | 93.70(9) | C(2)–Rh(2)–Rh(1) | 48.36(7) | | |
| C(4)–Rh(2)–Rh(1) | 49.86(6) | C(3)–Rh(2)–Rh(1) | 87.65(6) | C(2)–Rh(2)–Ru | 87.32(7) | | |
| C(4)–Rh(2)–Ru | 49.28(6) | C(3)–Rh(2)–Ru | 44.42(6) | Rh(1)–Rh(2)–Ru | 60.510(12) | | |
| O(1)–C(1)–Ru | 149.3(2) | O(1)–C(1)–Rh(1) | 127.1(2) | Ru–C(1)–Rh(1) | 83.56(9) | | |
| O(2)–C(2)–Rh(2) | 138.9(2) | O(2)–C(2)–Rh(1) | 137.2(2) | Rh(2)–C(2)–Rh(1) | 83.74(9) | | |
| O(3)–C(3)–Ru | 149.7(2) | O(3)–C(3)–Rh(2) | 126.9(2) | Ru–C(3)–Rh(2) | 83.47(9) | | |
| O(4)–C(4)–Rh(2) | 131.1(2) | O(4)–C(4)–Rh(1) | 131.0(2) | Rh(2)–C(4)–Rh(1) | 80.66(8) | | |
| O(4)–C(4)–Ru | 130.8(2) | Rh(2)–C(4)–Ru | 82.60(8) | Rh(1)–C(4)–Ru | 81.84(8) | | |

$CO)_3(\mu_3\text{-}CO)(\eta^5\text{-}C_5Me_5)_2(\eta^5\text{-}7,8\text{-}C_2B_9H_{11})]$ (**5**). As with many clusters containing multiple carbonyl ligands, it was difficult to elucidate the structure of the molecule from the spectroscopic data alone. Fortunately single crystals of **5** could be grown and an X-ray structure determination was carried out.

The molecule is shown in Fig. 3 and bond lengths and angles are given in Table 4. The molecule has a $RuRh_2$ triangular core [Ru–Rh(1) 2.7600(5), Ru–Rh(2) 2.7735(4), Rh(1)–Rh(2) 2.7030(5) Å] which is nearly equilateral as might be expected for adjacent second row transition metals. Complex **5** bears a significant resemblance to the cluster $[RuRh_2(\mu\text{-}CO)(\mu_3\text{-}CO)(CO)_2(\eta^4\text{-}C_8H_{10})(\eta^5\text{-}C_5Me_5)_2]$($C_8H_{10}$ = bicyclo[4.2.0]octa-2,4-diene) which contains a similar $RuRh_2$ triangle [Ru–Rh 2.766(1) and 2.815(1), Rh–Rh 2.672(1) Å] [30]. The ruthenium atom of **5**, however, is in a higher formal oxidation state ($Ru^{II}$) due to the carbaborane cage ligand. The latter which is pentahapto coordinated is not involved in exopolyhedral bonding to the trimetal core. The cage can be considered as occupying the position of the bicyclo[4.2.0]octa-2,4-diene ligand in $[RuRh_2(\mu\text{-}CO)(\mu_3\text{-}CO)(CO)_2(\eta^4\text{-}C_8H_{10})(\eta^5\text{-}C_5Me_5)_2]$.
The pentamethylcyclopentadienyl ligands in **5** ligate the Rh atoms [Rh(1)–C av. 2.246, Rh(2)–C av. 2.243 Å] with no significant slippage of either ring from an $\eta^5$ mode, as was similarly observed in the molecule $[RuRh_2(\mu\text{-}CO)(\mu_3\text{-}CO)(CO)_2(\eta^4\text{-}C_8H_{10})(\eta^5\text{-}C_5Me_5)_2]$.

Of particular note in **5** is the symmetrically capping $\mu_3$-C(4)O(4) group [Ru–C(4) 2.120(2), Rh(1)–C(4) 2.094(2), Rh(2)–C(4) 2.082(2) Å] to be compared with the $\mu_3$-CO ligand of $[RuRh_2(\mu\text{-}CO)(\mu_3\text{-}CO)(CO)_2(\eta^4\text{-}C_8H_{10})(\eta^5\text{-}C_5Me_5)_2]$ which shows a marked displacement away from the Ru atom towards the Rh atoms [Ru–C 2.247(4), Rh–C 2.038(4) and 2.069(4) Å]. The Rh(1)–Rh(2) bond in **5** is symmetrically bridged by C(2)O(2) [Rh(1)–C(2)–O(2) 137.2(2), Rh(2)-C(2)–O(2) 138.9(2)°] as occurs with the similar μ-CO ligand in $[RuRh_2(\mu\text{-}CO)(\mu_3\text{-}CO)(CO)_2(\eta^4\text{-}C_8H_{10})(\eta^5\text{-}C_5Me_5)_2]$. Moreover, in the Rh(μ-C)Rh bridge system of **5** the carbon–metal distances (av. 2.025 Å) are close in magnitude to those in $[RuRh_2(\mu\text{-}CO)(\mu_3\text{-}CO)(CO)_2(\eta^4\text{-}C_8H_{10})(\eta^5\text{-}C_5Me_5)_2]$ (av. 1.995 Å). The Ru–μ-C(O)–Rh carbonyl ligands of **5** can be construed as formally edge bridging (Ru–μ-C av. 1.954 Å, Rh–μ-C av. 2.192 Å), with the oxygen atoms clearly oriented towards the Rh atoms [Ru–C(1)–O(1) 149.3(2), Rh(1)–C(1)–O(1) 127.1(2), Ru–C(3)–O(3) 149.7(2), Rh(2)–C(3)–O(3) 126.9(2)°]. This is in contrast with $[RuRh_2(\mu\text{-}CO)(\mu_3\text{-}CO)(CO)_2(\eta^4\text{-}C_8H_{10})(\eta^5\text{-}C_5Me_5)_2]$ where only one Ru–Rh edge is semi-bridged by a CO molecule, the other CO molecule being terminally bound to the Ru atom [30].

The '$Ru(CO)_2(\eta^5\text{-}7,8\text{-}C_2B_9H_{11})$' unit is an $ML_5$ $d^6$ fragment, the cage occupying three positions of a distorted octahedron around the formally $Ru^{II}$ center.

With singly occupied $d_\pi$ and non-bonding $d_\sigma$ orbitals it can be considered as isolobal with a $CH_2$ moiety [23]. It is therefore not surprising that a stable trimer is formed in the reaction between **2** and the inorganic 'alkene' $[Rh_2(\mu\text{-}CO)_2(\eta^5\text{-}C_5Me_5)_2]$. The latter has been used previously in similar methodology to synthesize for example the complexes $[RuRh_2(\mu\text{-}CO)(\mu_3\text{-}CO)(CO)_2(\eta^4\text{-}C_8H_{10})(\eta^5\text{-}C_5Me_5)_2]$ [30], $[MoRh_2(\mu\text{-}CO)(CO)_5(\eta^5\text{-}C_5Me_5)_2]$ [31], $[PtRh_2(\mu\text{-}CO)_2(CO)(PPh_3)(\eta^5\text{-}C_5Me_5)_2]$ [32], and $[PtRh_4(\mu\text{-}CO)_4(\eta^5\text{-}C_5Me_5)_4]$ [33].

The IR spectrum of **5** displays a broad medium-intensity band at 1680 $cm^{-1}$ due to the $\mu_3$-CO group, this being within the accepted range for such triply bridging carbonyl ligands (1620–1730 $cm^{-1}$ [34]). The band at 1819 $cm^{-1}$ is likely due to the C(2)–O(2) group bridging the Rh(1)–Rh(2) bond with the remaining two bands (1852 and 1890 $cm^{-1}$) being attributable to C(1)–O(1) and C(3)–O(3) which span the Ru–Rh bonds though the frequencies are high for this type of CO. Compound **5** is sparingly soluble in common organic solvents and as a consequence the $^{13}C\{^1H\}$-NMR spectrum, which would have contained the most interesting spectroscopic data, was all but useless with just the $\eta^5\text{-}C_5Me_5$ ligands giving rise to observable signals. The $^1H$-NMR spectrum comprises two diagnostic singlets due to the $\eta^5\text{-}C_5Me_5$ and cage CH protons at $\delta$ 1.73 and 2.56 (30:2), respectively. The $^{11}B\{^1H\}$-NMR spectrum is as expected for a complex with a spectator carbaborane cage ligand.

Attempts were made to expand the use of **2** as a reagent to obtain mixed metal complexes via reactions with other metal–ligand fragments. Regrettably this was unsuccessful with the species $[Ti(Bu^n)_2(\eta^5\text{-}C_5H_5)_2]$, $[Mo(CO)_3(NCMe)_3]$, $[Mo_2(\mu\text{-}CO)_4(\eta^5\text{-}C_5Me_5)_2]$, $[Cu(THF)(\eta^5\text{-}C_5Me_5)]$, $[Pt(C_7H_{10})_3]$ and $[Pt(PEt_3)(C_7H_{10})_2]$ ($C_7H_{10}$ = norbornene). The primary drawback encountered in these reactions was the formation of highly stable species $[Ru(CO)_2L(\eta^5\text{-}7,8\text{-}C_2B_9H_{11})]$, where L is a ligand, generally CO, transferred from the other metal reagent. However, the ruthenium–platinum complex $[RuPt(\mu\text{-}H)(\mu\text{-}\sigma,\eta^5\text{-}7,8\text{-}C_2B_9H_{10})(CO)_2(PEt_3)_2]$, previously synthesized by treating [K(18-crown-6)]-$[RuH(CO)_2(\eta^5\text{-}7,8\text{-}C_2B_9H_{11})]$ with $[PtH(Cl)(PEt_3)_2]$ [2], was formed in good yield upon the reaction of **2** with $[Pt(PEt_3)_2(C_7H_{10})]$ in $CH_2Cl_2$.

## 3. Conclusions

The reagent **2** has proven a useful precursor for forming new ruthenacarbaborane–iron, –ruthenium, and –rhodium complexes. The species **3** make interesting additions to the family of Group 8 metal dimers **A**–**E**, while **4** and **5** are the result of a complex reaction where **5** is the expected product of the combination of the alkylidene-like fragment '$Ru(CO)_2(\eta^5\text{-}7,8\text{-}C_2B_9H_{11})$' and the alkene-like molecule $[Rh_2(\mu\text{-}CO)_2(\eta^5\text{-}C_5Me_5)_2]$.

## 4. Experimental

### 4.1. General considerations

All experiments were conducted under an atmosphere of dry nitrogen or argon using Schlenk-line techniques. Solvents were freshly distilled under nitrogen from appropriate drying agents before use. Petroleum ether refers to that fraction of boiling point 40–60°C. Tetrahydrofuran was distilled from K/benzophenone under nitrogen and stored over Na/K alloy. Chromatography columns (ca. 30 cm in length and 3 cm in diameter) were packed under nitrogen with silica gel (Acros 60–200 mesh). The NMR measurements were recorded at the following frequencies: $^1H$ 360.1, $^{13}C$ 90.6, and $^{11}B$ 115.3 MHz. IR spectra were measured with a Bruker IFS–25 spectrometer. The compounds $[NEt_4][RuI(CO)_2(\eta^5\text{-}7,8\text{-}C_2B_9H_{11})]$ (**1**) [2], $K[M(CO)_2(\eta^5\text{-}C_5H_5)]$ (M = Fe, Ru) [35] and $[Rh_2(\mu\text{-}CO)_2(\eta^5\text{-}C_5Me_5)_2]$ [36,37] were prepared as previously described.

### 4.2. Syntheses of the salts [K(18-crown-6)][cis-MRu(μ-CO)$_2$(CO)$_2$(η$^5$-C$_5$H$_5$)(η$^5$-7,8-C$_2$B$_9$H$_{11}$)] (M = Fe, Ru)

(a) Compound **1** (0.20 g, 0.37 mmol) was treated with $AgBF_4$ (0.08 g, 0.40 mmol) in THF (20 ml). After ca. 30 min, the mixture was filtered through a Celite pad to remove AgI and the yellow filtrate containing the reagent **2** was added dropwise to a THF (10 ml) solution of $K[Fe(CO)_2(\eta^5\text{-}C_5H_5)]$ (0.08 g, 0.37 mmol), prepared from $[Fe_2(CO)_4(\eta^5\text{-}C_5H_5)_2]$. After stirring at r.t. for 12 h, 18-crown-6 (0.11 g, 0.42 mmol) was added to the red solution. Solvent was then removed in vacuo and the residue chromatographed. Elution with $CH_2Cl_2$-THF (5:1) removed a red band, which on evaporation of the eluate in vacuo and crystallization from $CH_2Cl_2$-hexane (5 ml, 2:3), gave red crystals of [K(18-crown-6)][*cis*-$FeRu(\mu\text{-}CO)_2(CO)_2(\eta^5\text{-}C_5H_5)(\eta^5\text{-}7,8\text{-}C_2B_9H_{11})$] (**3a**) (0.06 g).

(b) In a similar manner $K[Ru(CO)_2(\eta^5\text{-}C_5H_5)]$ (0.10 g, 0.38 mmol) was treated with compound **2**, (generated in situ from **1** (0.20 g, 0.37 mmol)), followed by 18-crown-6 (0.11 g, 0.42 mmol) to yield yellow crystals of [K(18-crown-6)][*cis*-$Ru_2(\mu\text{-}CO)_2(CO)_2(\eta^5\text{-}C_5H_5)(\eta^5\text{-}7,8\text{-}C_2B_9H_{11})$] (**3b**) (0.06 g).

### 4.3. Reaction of [Ru(CO)$_2$(THF)(η$^5$-7,8-C$_2$B$_9$H$_{11}$)] with [Rh$_2$(μ-CO)$_2$(η$^5$-C$_5$Me$_5$)$_2$]

Excess $AgBF_4$ (ca. 0.08 g, 0.41 mmol) was added to the salt **1** (0.15 g, 0.28 mmol) in THF (20 ml). After 30 min, the solution was filtered through a Celite pad

Table 5
Data for X-ray crystal structure analyses

| | 3a | 5 |
|---|---|---|
| Crystal size (mm) | 0.40×0.35×0.10 | 0.20×0.15×0.15 |
| Empirical formula | $C_{23}H_{40}B_9FeKO_{10}Ru$ | $C_{26}H_{41}B_9O_4Rh_2Ru$ |
| $M_r$ | 769.86 | 821.77 |
| Crystal colour, shape | Red plate | Red prism |
| Crystal system | Triclinic | Monoclinic |
| Space group | $P\bar{1}$ | $P2_1/n$ |
| Temperature (K) | 173(2) | 173(2) |
| Unit cell dimensions | | |
| $a$ (Å) | 11.429(2) | 12.266(2) |
| $b$ (Å) | 11.450(3) | 14.510(2) |
| $c$ (Å) | 14.928(2) | 17.686(4) |
| $\alpha$ (°) | 92.01(2) | |
| $\beta$ (°) | 108.46(1) | 93.476(14) |
| $\gamma$ (°) | 114.17(8) | |
| $V$ (Å$^3$) | 1659.7(6) | 3141.9(9) |
| $Z$ | 2 | 4 |
| $D_{calc.}$ (g cm$^{-3}$) | 1.541 | 1.737 |
| $\mu$(Mo–K$_\alpha$) (mm$^{-1}$) | 1.067 | 1.545 |
| $F$(000) | 784 | 1632 |
| $2\theta$ range (°) | 5.0–50.0 | 3.6–55.0 |
| Reflections measured | 7896 | 19768 |
| Unique reflections | 5621 | 7172 |
| $R_{int}$ | 0.029 | 0.026 |
| Reflections limits | $-11\le h\le 13,\ -12\le k\le 13,\ -17\le l\le 16$ | $-15\le h\le 15,\ -12\le k\le 18,\ -22\le l\le 22$ |
| Final residuals | $wR_2=0.122$[a] ($R_1=0.045$)[b] | $wR_2=0.022$[a] ($R_1=0.050$)[b] |
| Weighting factors | $a=0.0836,\ b=0.0$[a] | $a=0.0214,\ b=0.0$[a] |
| Goodness of fit on $F^2$ | 0.96 | 0.96 |
| Final electron density difference features (max./min.) (e Å$^{-3}$) | 1.221, −1.374 | 0.591, −0.526 |

[a] Structure was refined on $F_o^2$ using all data: $wR_2=[\Sigma[w(F_o^2-F_c^2)^2]/\Sigma w(F_o^2)^2]^{1/2}$ where $w^{-1}=[\sigma^2(F_o)^2+(aP)^2+bP]$ and $P=[\max(F_o^2,0)+2F_c^2]/3$.

[b] The value in parentheses is given for comparison with refinements based on $F_o$ with a typical threshold of $F_o>4\sigma(F_o)$ and $R_1=\Sigma||F_o|-|F_c||/\Sigma|F_o|$ and $w^{-1}=[\sigma^2(F_o)+gF_o^2]$.

directly onto the blue solid [$Rh_2(\mu\text{-}CO)_2(\eta^5\text{-}C_5Me_5)_2$] (0.15 g, 0.28 mmol) and within 15 min, the blue solution had turned purple–red to green in color. This green solution was stirred at r.t. for 2 h before being refluxed for 1 h. The solution was then filtered through Celite to remove a small amount of a black precipitate and then excess solvent was removed in vacuo. The resulting solution was chromatographed at −30°C, eluting initially with $CH_2Cl_2$–light petroleum (2:3). A red band was removed from the column, from which solvent was removed in vacuo and crystallization from $CH_2Cl_2$–light petroleum (5 ml, 2:3) gave red microcrystals of [$RuRh(\mu\text{-}H)(\mu\text{-}\sigma,\eta^5\text{-}7,8\text{-}C_2B_9H_{10})(CO)_3(\eta^5\text{-}C_5Me_5)$] (**4**) (0.03 g). Further elution with the same solvent mixture removed more red material, which was shown to contain primarily complex **4**. Increasing the polarity of the eluting solvent ($CH_2Cl_2$–light petroleum (1:1)) removed a broad dark green fraction. Evaporation of solvent in vacuo and crystallization from $CH_2Cl_2$–light petroleum (10 ml, 1:4) yielded dark green microcrystals of [$RuRh_2(\mu\text{-}CO)_3(\mu_3\text{-}CO)(\eta^5\text{-}C_5Me_5)_2(\eta^5\text{-}7,8\text{-}C_2B_9H_{11})$] (**5**) (0.09 g).

### 4.4. X-ray structural analyses

Crystals of **3a** and **5** were grown by diffusion of *n*-hexane (**3a**) or light petroleum (**5**) into $CH_2Cl_2$ solutions of the complexes. The crystals were mounted on glass fibers and low-temperature data were collected on a Siemens SMART CCD area-detector 3-circle diffractometer using Mo–K$_\alpha$ X-radiation, $\bar{\lambda}=0.71073$ Å. For three settings of $\phi$, narrow data 'frames' were collected for 0.3° increments in ω. A total of 1321 frames of data were collected affording rather more than a hemisphere of data. At the end of data collection the first 50 frames of data were recollected confirming that crystal decay had not taken place during the course of data collection. The substantial redundancy in data allows empirical absorption corrections to be applied using multiple measurements of equivalent reflections (SADABS) [38]. Data frames were collected for 20 s (**3a**) and 10 s (**5**) per frame. The data frames were integrated using SAINT [38] and the structures were solved by conventional direct methods. The structures were refined by full-matrix least-squares on all $F^2$ data using Siemens SHELXTL ver. 5.03 [38], with anisotropic thermal parameters for all non-hydrogen atoms. All hydrogen atoms were included in calculated positions and allowed to ride on the parent boron or carbon atoms with isotropic thermal parameters ($U_{iso}=1.2\times U_{iso\ equiv.}$ of the parent atom except for Me protons where $U_{iso}=1.5\times U_{iso\ equiv.}$). One of the carbon atoms of the 18-crown-6 ligand in **3a** was disordered over two sites [C(32A) (36%) and C(32B) (64%)]. All calculations were carried out on Silicon Graphics Iris, Indigo, or Indy computers. Experimental data are recorded in Table 5.

## 5. Supplementary material

Atomic coordinates, a complete listing of bond lengths and angles, and the thermal parameters have been deposited at the Cambridge Crystallographic Data Centre (deposition numbers CCDC 104121 (**3a**) and CCDC 104122 (**5**)).

## Acknowledgements

We thank the Robert A. Welch Foundation for support (Grant AA-1201) and Dr James Karban for

running the $^{11}B\{^1H\}-^{11}B\{^1H\}$-COSY-NMR spectrum of **4**.

## References


[1] For leading refs. see: M.A. Bennett, K. Khan, E. Wenger, in: E.W. Abel, F.G.A. Stone, G. Wilkinson (Eds.), Comprehensive Organometallic Chemistry II, vol. 7, Pergamon Press, Oxford, 1995, pp. 473–548.
[2] S. Anderson, D.F. Mullica, E.L. Sappenfield, F.G.A. Stone, Organometallics 14 (1995) 3516.
[3] S. Anderson, D.F. Mullica, E.L. Sappenfield, F.G.A. Stone, Organometallics 15 (1996) 1676.
[4] S. Anderson, J.C. Jeffery, Y.-H. Liao, D.F. Mullica, E.L. Sappenfield, F.G.A. Stone, Organometallics 16 (1997) 958.
[5] J.C. Jeffery, P.A. Jelliss, Y.-H. Liao, F.G.A. Stone, J. Organomet. Chem. 551 (1998) 27.
[6] J.C. Jeffery, P.A. Jelliss, E. Psillakis, G.E.A. Rudd, F.G.A. Stone, J. Organomet. Chem. 562 (1998) 17.
[7] P.E. Behnken, M.F. Hawthorne, Inorg. Chem. 23 (1984) 3420.
[8] B.P. Gracey, S.A.R. Knox, K.A. Macpherson, A.G. Orpen, S.R. Stobart, J. Chem. Soc. Dalton Trans. (1985) 1935.
[9] I. Blandford, J.C. Jeffery, P.A. Jelliss, F.G.A. Stone, Organometallics 17 (1998) 1402.
[10] For leading refs. see W.P. Fehlhammer, H. Stolzenberg, in: E.W. Abel, F.G.A. Stone, G. Wilkinson (Eds.), Comprehensive Organometallic Chemistry, vol. 4, Pergamon Press, Oxford, 1982, pp. 514–518.
[11] R.F. Bryan, P.T. Greene, J. Chem. Soc. (A) (1970) 3064.
[12] R.F. Bryan, P.T. Greene, M.J. Newlands, D.S. Field, J. Chem. Soc. (A) (1970) 3068.
[13] For leading refs. see M.A. Bennett, M.I. Bruce, T.W. Matheson, in: E.W. Abel, F.G.A. Stone, G. Wilkinson (Eds.), Comprehensive Organometallic Chemistry, vol. 4, Pergamon Press, Oxford, 1982, pp. 823–825.
[14] O.S. Mills, J.P. Nice, J. Organomet. Chem. 9 (1967) 339.
[15] R.F. Bryan, P.T. Greene, Inorg. Chem. 9 (1970) 1464.
[16] R.T. Sanderson, Chemical Periodicity, Reinhold, New York, 1960, p. 28.
[17] A. Bondi, J. Phys. Chem. 68 (1964) 441.
[18] J.L. Cihonski, R.A. Levenson, Inorg. Chem. 14 (1975) 1717.
[19] M.K. Cooper, P.A. Duckworth, K. Henrick, M. McPartlin, J. Organomet. Chem. 212 (1981) C10.
[20] (a) W.F. Edgell, J. Lyford, A. Barbetta, C.I. Jose, J. Am. Chem. Soc. 93 (1971) 6403. (b) W.F. Edgell, J. Lyford, J. Am. Chem. Soc. 98 (1976) 2434.
[21] K.H. Pannell, D. Jackson, J. Am. Chem. Soc. 98 (1976) 4443.
[22] M.F. Hawthorne, H.W. Ruhle, Inorg. Chem. 8 (1969) 176.
[23] R. Hoffmann, Angew. Chem. Int. Ed. Engl. 21 (1982) 711.
[24] J.G. Bullitt, F.A. Cotton, T.J. Marks, Inorg. Chem. 11 (1972) 671.
[25] R.D. Adams, Y. Chi, D.-K. Hwang, L.J. Farrugia, in: E.W. Abel, F.G.A. Stone, G. Wilkinson (Eds.), Comprehensive Organometallic Chemistry II, vol. 10, Pergamon Press, Oxford, 1995, pp. 1–22, 85–185, 187–254.
[26] H.-C. Boettcher, M. Graf, K. Merzweiler, J. Organomet. Chem. 534 (1997) 43.
[27] T. Nakajima, I. Shimizu, K. Kobayashi, Y. Wakatsuki, Organometallics 17 (1998) 262.
[28] A. Fumagalli, M. Bianchi, M.C. Malatesta, G. Ciani, M. Moret, A. Sironi, Inorg. Chem. 37 (1998) 1324 and references cited therein.
[29] H.D. Kaesz, R.B. Saillant, Chem. Rev. 72 (1972) 231.
[30] L.J. Farrugia, J.C. Jeffery, C. Marsden, F.G.A. Stone, J. Chem. Soc. Dalton Trans. (1985) 645.
[31] R.D. Barr, M. Green, J.A.K. Howard, T.B. Marder, F.G.A. Stone, J. Chem. Soc. Dalton Trans. (1984) 2757.
[32] M. Green, R.M. Mills, G.N. Pain, F.G.A. Stone, P. Woodward, J. Chem. Soc. Dalton Trans. (1982) 1321.
[33] M. Green, J.A.K. Howard, G.N. Pain, F.G.A. Stone, J. Chem. Soc. Dalton Trans. (1982) 1327.
[34] Ch. Elschenbroich, A. Salzer, Organometallics: A Concise Introduction, 2nd ed., VCH, Weinheim, 1992, p. 229.
[35] J.S. Plotkin, S.G. Shore, Inorg. Chem. 20 (1981) 284.
[36] A. Nutton, P.M. Maitlis, J. Organomet. Chem. 166 (1979) C21.
[37] M.L. Aldridge, M. Green, J.A.K. Howard, G.N. Pain, S.J. Porter, F.G.A. Stone, P. Woodward, J. Chem. Soc. Dalton Trans. (1982) 1333.
[38] Siemens X-ray Instruments, Madison, WI.